



Contents lists available at ScienceDirect

Optik

journal homepage: [www.elsevier.com/locate/ijleo](http://www.elsevier.com/locate/ijleo)

Original research article

# Impact analysis of lens shutter of aerial camera on image plane illuminance

Xianfeng Li<sup>a,b,\*</sup>, Huibin Gao<sup>a</sup>, Chunfeng Yu<sup>a</sup>, ZhiChao Chen<sup>a</sup><sup>a</sup> Changchun Institute of Optics, Fine Mechanics and Physics, Chinese Academy of Sciences, Changchun 130033, China<sup>b</sup> University of Chinese Academy of Sciences, Beijing 100049, China

## ARTICLE INFO

## Keywords:

Lens shutter  
Luminous flux  
Transfer function  
Photoelectric measurement  
Image plane illuminance

## ABSTRACT

In order to obtain high resolution aerial images, in addition to adopt high transfer function of optical system and high quality imaging medium, the exposure time of the shutter should be properly controlled, so as to make sure the appropriate exposure of the CCD sensor. The paper applies an aerial mapping camera shutter the structure and working principle of the mirror, presents the mirror shutter algorithm of the working period of luminous flux, on the basis of radiation theory. The paper also analyze the transfer relations of the object and image of the light energy on the optical system with large field of view, short focal length and large relative aperture. The experimental results show that the illumination precision of image plane improved by 8.9%, compared with the traditional algorithm and the gain exposure of CCD sensor is closer to the actual light energy. In addition, these design can also provide theoretical reference for image uniformity correction, CCD gain adjustment and variable density neutral filter processing.

## 1. Introduction

Aerial photography is an important means to obtain the target information [1]. As a device to control exposure, the shutter is an important part of aerospace camera. If the quantity of exposure can not be properly controlled [2], high resolution images will not be obtained. The overexposure or underexposure will lead to loss of target information, and camera performance and function will not play well.

Based on the development of the digital aerial photography camera, the edge illuminance of content mirror surface with large field of view relatively seriously decline, compared with center of the optical system. In order to improve the resolution of image edge, exposure has to be increased 2–3 times, which will lead to the inner part of the field exposure, uniformity, lower contrast and declined image quality. In order to improve the field image quality, the changed density plating membrane filter is usually applied in optical system, which reduce the inner part of the photo exposure two-thirds in the center and almost none in the corner [3]. Although this process can reach the requirement of uniform illumination, but lost a part of light energy, reduces the image plane illumination value. Therefore, it is necessary to analyze the impact of the shutter working process on the surface illumination based on radiation theory [4].

## 2. Structure design of shutter

Combining with the camera shutter operating characteristics and technical parameters, we develop a aerial shutter mechanism

\* Corresponding author.

E-mail address: [pioneer@126.com](mailto:pioneer@126.com) (X. Li).<https://doi.org/10.1016/j.ijleo.2018.07.076>

Received 19 May 2018; Accepted 20 July 2018

0030-4026/© 2018 Published by Elsevier GmbH.



Fig. 1. Photograph of Shutter.

between the mirror. The shutter has a wide range to adjust exposure time, high optical efficiency and adjustable exposure time [5].

The target camera belongs to the type of surveying and mapping camera, so the shutter can't affect the calibration precision of inside azimuth element. Therefore, we can only adopt the central type shutter. The shutter is mainly composed of blade, slow shutter shell, transmission gear train and drive motor and so on. The material object of shutter is shown in Fig. 1. The shutter controls the rotation of the blade so that the opening of the fast blade and the slow blade is exposed by the light beam.

The fast blade controls the exposure time, and the slow blade controls the exposure cycle, which is equivalent to the light brake.

### 2.1. Design of shutter-blade

The air gap between the lens group of the optical system is quite small, and the aperture stop is also placed in the middle of the air gap location. So the distance between the blade and the aperture stop and lens group is only 0.4 mm. In order to ensure the reliability and service life of the shutter structure requirement, the rotational inertia of the blade and shaft parts must be reduced. So the shutter blade material compose of high elastic modulus carbon fiber composite material [6]. The 3D model of the blade is shown in Fig. 2.

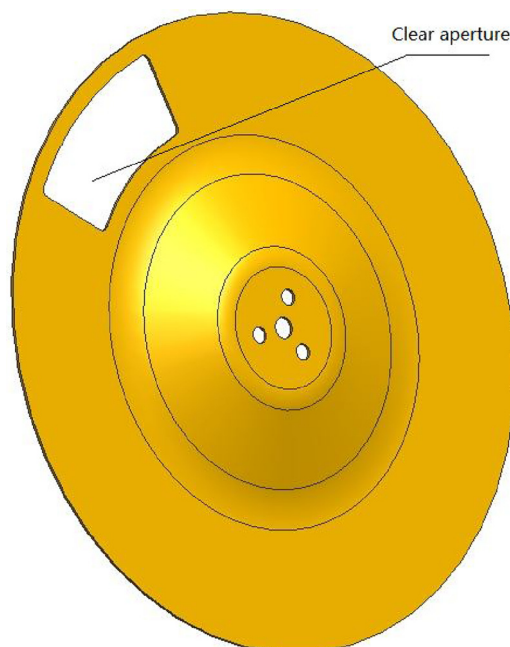


Fig. 2. Three-dimensional Model of Shutter-blade.

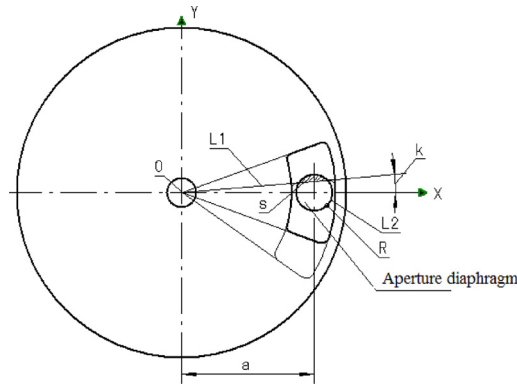


Fig. 3. Schematic diagram of blade scanning aperture.

2.2. Efficiency of shutter

The shutter must have a high optical efficiency to ensure the image quality of the camera. The shutter is divided into the opening stage, the full opened stage and the closing stage in the whole exposure time. According to the definition of the shutter efficiency, the calculation formula of shutter efficiency is as follows:

$$\eta = \frac{\int_{t_0}^{t_1} E(t)d(t) + \int_{t_1}^{t_2} E(t)d(t) + \int_{t_2}^{t_3} E(t)d(t)}{Et_\varphi} = \frac{t_0\eta_0 + t_1\eta_1 + t_2\eta_2}{t_\varphi} = \frac{t_e}{t_\varphi} \tag{1}$$

where  $\eta$  is the shutter efficiency,  $E$  is the illumination of the focal plane,  $t_\varphi$  is the actual exposure time,  $t_e$  is effective exposure time.  $\eta_0$  is the opening stage shutter efficiency on the opening stage.  $\eta_1$  the shutter efficiency on the full opened stage,  $\eta_2$  is the shutter efficiency on the shutoff stage.  $t_0$  is the time during the opening stage,  $t_1$  is the time during the full opened stage,  $t_2$  is the time during the closing time.

The exposure process of the photosensitive device can be converted into the working characteristic curve of the shutter, which can directly describe the change of the luminous flux over time during the exposure process of the optical system. Assuming the target luminance is uniform, the change of aperture area along with the change of time can take place of the quantity of light pass. During the working period of lens shutter, the changes of the aperture diaphragm area is shown in Fig. 3. Zero point is the origin of coordinate system, which is the blade rotation axis. And  $R$  is the radius of the aperture diaphragm.

According to the change of the aperture diaphragm area  $S$  with time  $t$ , the working characteristic curve of the shutter can be drawn directly, as shown in Fig. 4, the time from 0 to  $T_0$  is the stage of the shutter preparation exposure.

It can be seen from the shutter characteristic curve that the opening and closing stages of the shutter are symmetrical during the whole exposure cycle.

3. Illuminance on the image surface of object lens

When the optical system image the object, the illuminance of image point outside the axis is lower than the illuminance on the axis, even without vignetting [7]. The illuminance of image point on the axis usually satisfies the law of the fourth power of the cosine, and the formula is as follows:

$$E_0 = \frac{n^2}{n^2} \pi L \tau \sin^2(u') = \pi L \tau u'^2 = \pi L \tau \left(\frac{D}{2f}\right)^2 = \frac{\pi L \tau}{4F^2} \tag{2}$$

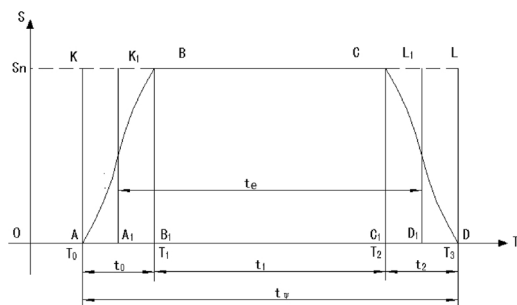


Fig. 4. Characteristic curve of the shutter.

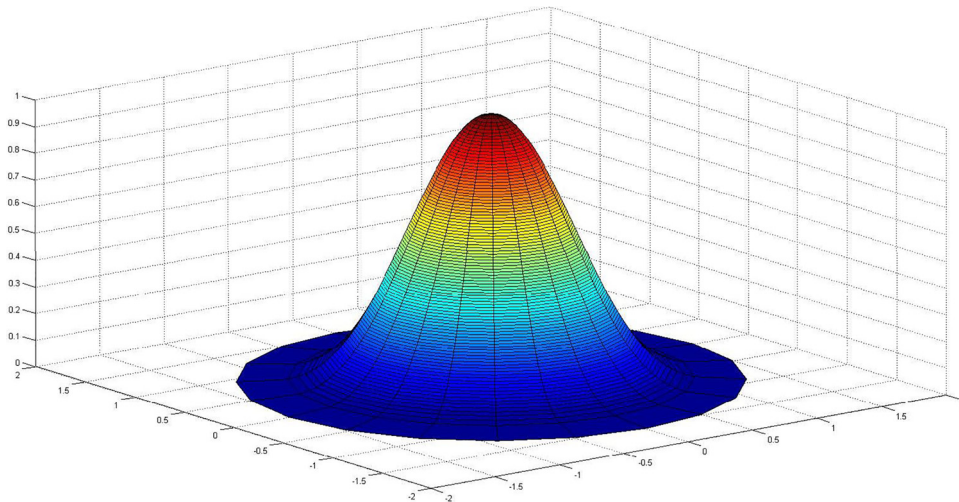


Fig. 5. Curve of illumination on the image surface of objective lens.

On the plane of exit pupil, when the aberration is equilibrium or minimum, the illuminance of image point outside the axis is as follows:

$$E = E_0 \cos^4(w) = \frac{\pi L \tau}{4F^2} \cos^4(w) \tag{3}$$

According to Eq. (3), the illuminance with different views of angles of image point outside the axis is compared with that of on the axis. The illumination function mapping of the image plane is shown in Fig. 5. According to Fig. 5, evidently the illuminance of outside the axis rapidly decreased with the increase of the view of angle. For the optical system of digital aerial photographic camera, the illumination of the edge field is 68% lower than that of the center field, and the decrease is very serious. This analysis is based on that aperture diaphragm is circular and the decreasing is proportional to the biquadrate of the diameter of the aperture. In fact, in the process of scanning the aperture diaphragm shutter blades incision, the aperture diaphragm change is not round, but irregular shape [8]. So we need analyze the process of the shutter work and its impact on the image plane illumination based on the theory of luminous flux.

### 3.1. Analysis of light flux

The optical system of digital aerial photography camera can be considered as an aplanatic points optical system on which spherical aberration and vignetting is fully calibrated [9]. Assuming that surface reflection, absorption and scattering losses of light radiation don't happen on the optical system, and the object is lambert cosine radiator, then the diagrammatic representation of stereoscopic angle corresponding to angle increment is shown as Fig. 6.

The shaded area in the Fig. 6 is the aperture area of aperture stop in plane of the entrance pupil.  $dA$  is the micro-luminescence area of the point on the object space on the axis. The three-dimensional Angle mathematical model which constitute of the beam of radiation from  $dA$  to the entrance pupil is established and  $dA$  is the origin of coordinates.

According to the radiation theory, the light flux of the Lambertian radiator emitted to the solid Angle corresponding to the planar

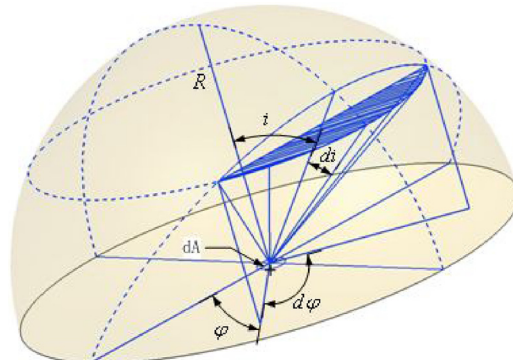


Fig. 6. Sketch map of solid Angle corresponds to the angle increment.

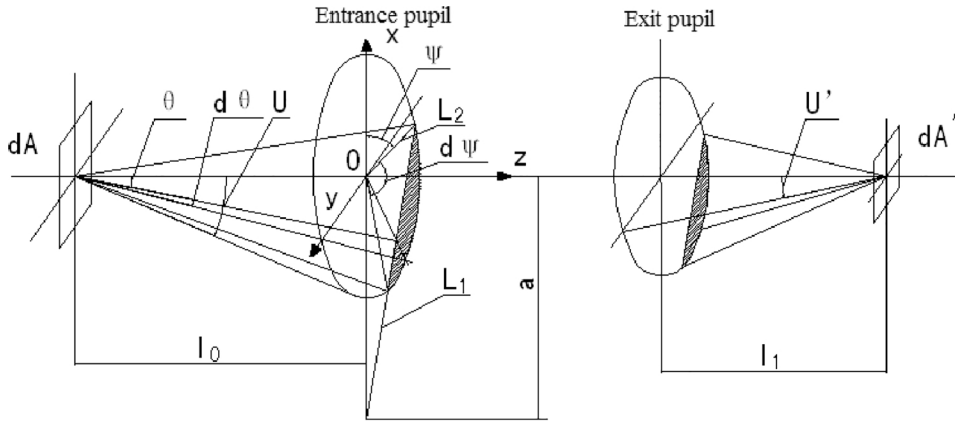


Fig. 7. Illumination on the axis of optical system.

aperture angle  $U$  on the plane of entrance pupil is:

$$\phi = LdA \int_{\psi_1}^{\psi_2} \int_{\theta=U(k)}^{\theta=U} \sin(\theta)\cos(\theta)d\theta d\psi \tag{4}$$

3.2. Illumination of image point on the axis

To analyze the optical system of digital aerial photography camera, the mathematical model is established for the intersection point of the entrance pupil surface and the optical axis as a origin. The shaded region is the region where the light passes through, as is shown in Fig. 7. O is the origin of cartesian coordinates. The distance from the center of the blade to the optical axis is  $a$ . The Angle between the ligature from arbitrarily point of the line  $L_1$  to the point on the axis and the optical axis is  $\theta$ .  $dA$  and  $dA'$  respectively represent the small area of the object and the image near the axis. The aperture Angle of the object is  $U$ . The aperture angle of the image is  $U'$ . The light brightness of the object surface and the image surface is  $L$  and  $L'$ .

When the distance  $l_0$  between the Lambertian radial body and the entrance pupil is infinite, compared with diameter of entrance pupil. The luminous surface can take place of the sphere to calculate the solid angle of. According to the principle of calculus, the light flux emitted from Lambertian radiation body with the solid angle  $U$  in the surface of entrance pupil is obtained through mathematical model and Eq. (4), and the equation of the equation  $L_1$  is as follows:

$$y = k(x + a) \begin{cases} 0 \leq k \leq \tan(\frac{R}{\sqrt{a^2 - R^2}}); \\ -\tan(\frac{R}{\sqrt{a^2 - R^2}}) \leq k \leq 0; \end{cases} \tag{5}$$

In the Eq. (5),  $R$  is the pupil radius;  $k$  is the slope of the line equation  $L_1$ ;  $a$  is the distance from the center of the blade to the optical axis.

There are two kinds of linear equation in the blade incision. Each of them has a gap point, but it is the first kind of discontinuity point. When the minimum value  $k$  is taken, the aperture stop is closed; When the maximum value  $k$  is taken, the aperture stop is fully open; When the zero value  $k$  is taken, the aperture stop is half open.

The entrance pupil equation  $L_2$  is :

$$x^2 + y^2 = R^2 \tag{6}$$

According to Fig. 8, the variation range of the Angle  $\psi$  can be obtained as follows:

$$\psi_1 = \arctan(\frac{y_1}{x_1}) = \arctan(\frac{ak + 2ak^3 + k\sqrt{R^2(1+k^2) - k^2a^2}}{ak^2 + \sqrt{R^2(1+k^2) - k^2a^2}})$$

$$\psi_2 = \arctan(\frac{y_2}{x_2}) = \arctan(\frac{ak + 2ak^3 - k\sqrt{R^2(1+k^2) - k^2a^2}}{ak^2 - \sqrt{R^2(1+k^2) - k^2a^2}})$$

The maximum value of  $\theta$  angle is the aperture Angle of the object. Its value is:

$$U = \arctan(\frac{R}{l_0})$$

The equation of the line which passes through the origin of the frame and intersects the line  $L_1$  is:

$$y = \tan(\psi)x \tag{7}$$

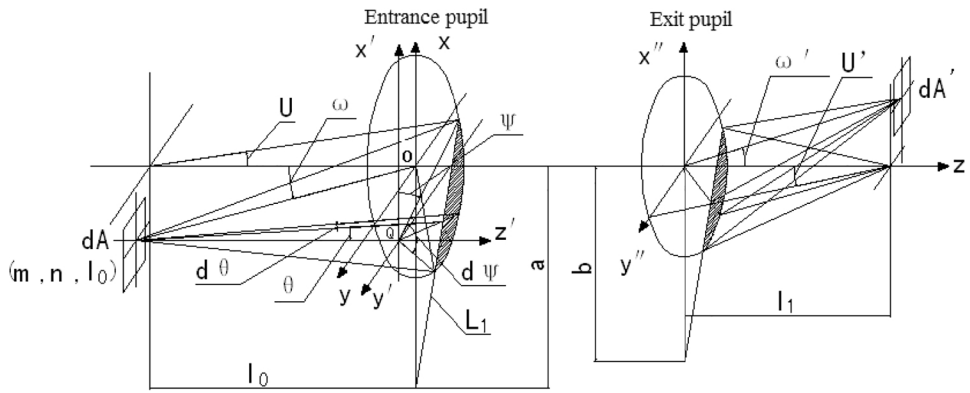


Fig. 8. Illuminance of point outside the axis of optical system.



Fig. 9. The measurement of illuminance on the image surface of camera.



Fig. 10. The picture of the half-opened aperture.

The corresponding  $\theta$  angle at any point on the line  $L_1$  is:

$$\theta = \arctan\left(\frac{\sqrt{x^2 + y^2}}{l_0}\right) = \arctan\left(\frac{ak}{l_0 \sin(\psi) - kl_0 \cos(\psi)}\right)$$

According to Eq. (4), the luminous flux emitted by the point on the axis during the stereoscopic angle range of the entrance pupil can be obtained:

$$\begin{aligned} \phi &= LdA \int_{\psi_1}^{\psi_2} \int_{\theta=U(k)}^{\theta=U} \sin(\theta) \cos(\theta) d\theta d\psi \\ &= \frac{1}{2} LdA (\sin^2(ac \tan(\frac{R}{l_0}))(\psi_2 - \psi_1) - a^2 k^2 \int_{\psi_1}^{\psi_2} \frac{1}{a^2 k^2 + l_0^2 (\sin(\psi) - k \cos(\psi))^2} d\psi) \end{aligned}$$

**Table 1**  
Local gray scale.

	1	2	3	4	5	6	7	8	9	10
1	2716	2456	2224	2088	2524	2972	2172	1812	2912	2604
2	2964	1936	2096	2076	1968	1644	2720	2840	2004	2036
3	2168	1968	2272	1968	2692	4916	2348	3372	2264	2372
4	2688	2072	2900	1984	2720	2364	1816	2036	2800	1960
5	2392	2452	2092	1976	2480	1972	2088	2028	2316	2760
6	2108	2196	2460	3312	2328	2460	2864	3184	2132	2616
7	2160	2532	2004	2356	2200	2568	2332	2652	2140	2332
8	2584	2040	2844	2860	2652	2464	2116	1948	2052	2552
9	2312	2352	2104	2380	2052	2600	2892	1976	1964	2484
10	2684	2924	3040	2492	2960	3336	2496	2564	2328	2208
11	3196	2592	2132	2696	2352	2088	2376	2052	3688	2600
12	2216	2108	4008	2168	2888	2472	2168	2200	2596	3692
13	2596	2216	2556	2760	2048	2664	2188	2272	2464	2612
14	2712	2504	2168	2064	2592	2712	2256	3320	2248	2844
15	1984	2372	2060	2368	2048	3340	2264	2756	2856	3380
16	2776	2424	3256	2048	2180	2212	2800	2156	2352	2636
17	3476	2136	2052	2036	2976	2248	2196	2616	2824	2432
18	2228	3252	2628	2088	2284	2572	2584	2976	2048	2196
19	2804	2268	2272	2128	2520	2188	2136	2508	2240	2308
20	2656	2260	2264	2748	2444	2712	2444	2708	2748	2840
22	2644	2504	2344	2656	2528	2840	2524	2016	2472	3016
23	2236	3336	2468	2660	2496	3044	2408	3012	2748	2508
24	2252	2376	2256	2156	2756	2072	3316	2676	2664	2304
25	2716	2356	2596	2640	2656	2764	2784	2332	2572	2568

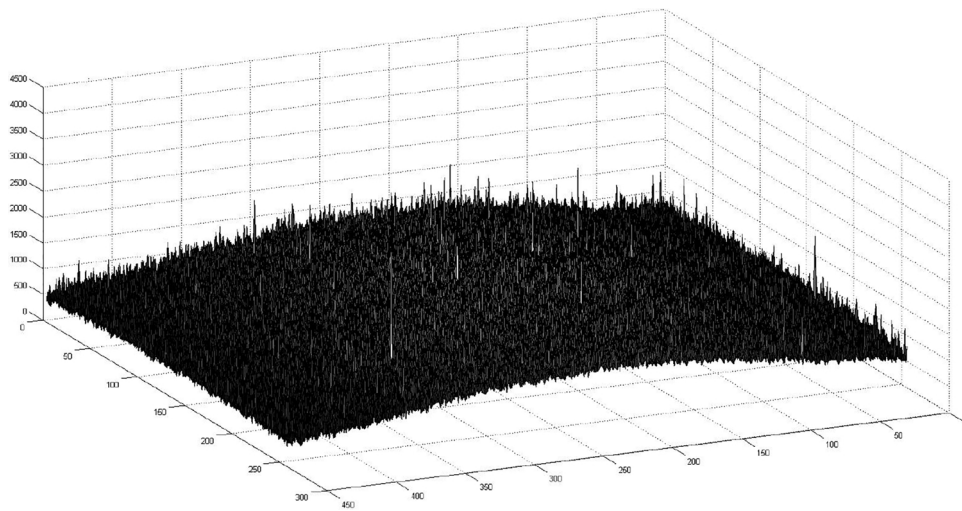


**Fig. 11.** Three dimensional gray surface.

If the transmission ratio of the optical system is  $\tau_g$ , the vertical power of the vertical axis is  $\beta$ , the refractive index of the object and image space is equal, and the illuminance of the image points on the axis is as follows:

$$E'_0 = \frac{\phi'}{dA'} = \frac{1}{2} \frac{\tau_g L}{\beta^2} \left( \frac{R^2}{l_0^2 + R^2} (\psi_2 - \psi_1) - \sqrt{\frac{a^2 k^2}{a^2 k^2 + l_0^2 + l_0^2 k^2}} \left( \arctan \left( \sqrt{\frac{a^2 k^2 + l_0^2 + l_0^2 k^2}{a^2 k^2}} \tan(2\psi_2 - 2\delta) \right) - \arctan \left( \sqrt{\frac{a^2 k^2 + l_0^2 + l_0^2 k^2}{a^2 k^2}} \tan(2\psi_1 - 2\delta) \right) \right) \right)$$

The function relation between the illuminance of the image point on the axis and the opening time of aperture stop and the rotation angular velocity of the blade is established, as is shown as:

$$E'_0 = I_1(l_0, R, k, a) - I_2(l_0, R, k, a) + I_3(l_0, R, k, a) \tag{8}$$

Among them:

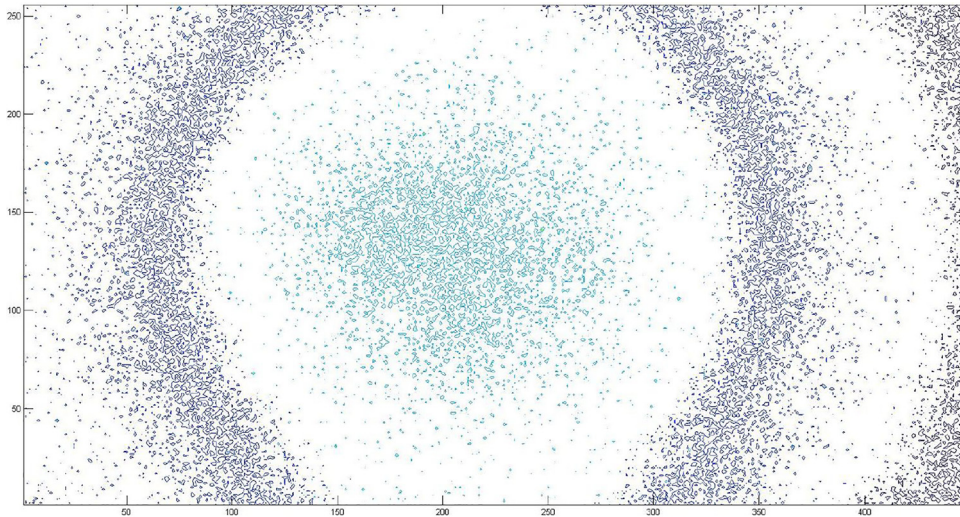


Fig. 12. Grayscale contour map.

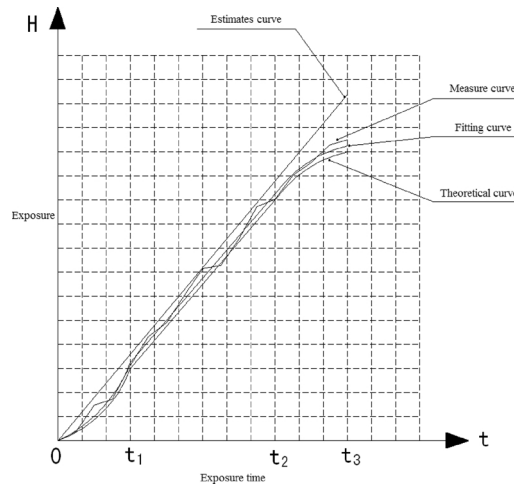


Fig. 13. Curve which exposure varies with time.

$$I_1(l_0, R, k, a) = \frac{1}{2} \tau_g L \sin^2(U') (\psi_2 - \psi_1);$$

$$I_2(l_0, R, k, a) = \frac{\tau_g L \sin^2(U') (l_0^2 + R^2)}{2R^2} \frac{ak}{\sqrt{a^2 k^2 + l_0^2 + l_0^2 k^2}} \arctan\left(\frac{\sqrt{a^2 k^2 + l_0^2 + l_0^2 k^2}}{ak} \tan(2\psi_2 - 2\delta)\right)$$

$$I_3(l_0, R, k, a) = \frac{\tau_g L \sin^2(U') (l_0^2 + R^2)}{2R^2} \frac{ak}{\sqrt{a^2 k^2 + l_0^2 + l_0^2 k^2}} \arctan\left(\frac{\sqrt{a^2 k^2 + l_0^2 + l_0^2 k^2}}{ak} \tan(2\psi_1 - 2\delta)\right)$$

As shown in Eq. (8), the intensity of illumination of image point on the axis is directly proportional to sine the sum of the squares of sine of aperture angle and the time of the opening of the aperture stop, and is inversely proportional to the square of the vertical shaft power, distance of the object surface to the entrance pupil and the angular velocity of the blade rotation. The illumination of the image points on the axis of the opening stage of aperture stop is as follows:

$$E_1 = \int_{T_0}^{T_1} E'_0 dt = \int_{T_0}^{T_1} I_1(l_0, R, k, a) dt - \int_{T_0}^{T_1} I_2(l_0, R, k, a) dt + \int_{T_0}^{T_1} I_3(l_0, R, k, a) dt$$

The illumination of the image points on the axis of the full opened stage of aperture stop is as follows:

$$E_2 = E'_0 t_1 = I_1(l_0, R, k, a) t_1 - I_2(l_0, R, k, a) t_1 + I_3(l_0, R, k, a) t_1$$

The illuminance of the image points on the axis of the closing stage of aperture stop of aperture is:

$$E_3 = \int_{T_2}^{T_3} E'_0 dt = \int_{T_2}^{T_3} I_1(l_0, R, k, a) dt - \int_{T_2}^{T_3} I_2(l_0, R, k, a) dt + \int_{T_2}^{T_3} I_3(l_0, R, k, a) dt$$

In the shutter release cycle, the process of opening and closing the aperture stop is symmetrical, and the illuminance on the axis is as follows:

$$E_0 = 2E_1 + E_2$$

### 3.3. Illumination of image point outside the axis

The imaging of the image outside the axis is more complex than the image on the axis. There is an Angle  $\omega'$  between the main light of the small area  $dA'$  outside the axis and the optical axis. This is the Angle of view of the external image point. Its existence makes the square aperture of the outer point of the axis is smaller than that of the square aperture of on the axis, and the illuminance of the external image point is lower than that of the point on the axis. The illuminance of the external image point can be obtained by means of moving coordinate system. A mathematical model is established for the intersection of the entrance pupil surface and the optical axis, and the shaded region is the region where the light passes through, as is shown in Fig. 8.

The equation of line  $L'$  in frame  $x'y'z'$  is:

$$y' = k(x' + m + a) - n \begin{cases} 0 \leq k \leq \tan(\frac{R}{\sqrt{a^2 - R^2}}); \\ -\tan(\frac{R}{\sqrt{a^2 - R^2}}) \leq k \leq 0; \end{cases} \tag{9}$$

The equation of entrance pupil  $L_2$  in frame  $x'y'z'$  is as follows:

$$(x' + m)^2 + (y' + n)^2 = R^2 \tag{10}$$

In the Eq. (10),  $R$  is the radius of entrance pupil,  $k$  is the slope of the line equation  $L_1$ ,  $a$  is the distance from the center of the blade to the optical axis. The range of the angle  $\theta$  can also be obtained. But the maximum value of the angle  $\theta$  is not the aperture angle of the object, on the contrary it is determined by the intersection of the equation of the line through the origin of the coordinate system and the entrance pupil equation.

The equation of the line  $L_3$  through the origin of frame  $x'y'z'$  and the through-light region is:

$$y' = \tan(\psi)x' \tag{11}$$

After the intersection point is obtained, the luminous flux emitted by the outer point of the axis during the stereoscopic Angle range of the entrance pupil can be obtained.

$$\begin{aligned} \phi &= LdA \int_{\psi_1}^{\psi_2} \int_{\theta_1}^{\theta_2} \sin(\theta)\cos(\theta)d\theta d\psi \\ &= \frac{1}{2}LdA \left( \int_{\psi_1}^{\psi_2} \sin^2(\arctan(\cos(\psi) \frac{\tan(\psi)n + m + \sqrt{(R^2 - m^2)\tan^2(\psi) + 2\tan(\psi)mn + R^2 - n^2}}{l_0}})) d\psi - \right. \\ &\quad \left. \sin^2(\arctan(\frac{km + ka - n}{l_0 \sin(\psi) - kl_0 \cos(\psi)})) d\psi \right) \end{aligned}$$

The top formula can be divided into two parts  $J_1(l_0, R, m, n, k, a)$  and  $J_2(l_0, R, m, n, k, a)$ , and the integral operating is done separately.

$$\begin{aligned} J_1(l_0, R, m, n, k, a) &= \frac{1}{2}LdA((\psi_2 - \psi_1) - \\ & l_0^2 \int_{\psi_1}^{\psi_2} \frac{1}{l_0^2 + (\sqrt{n^2 + m^2} \cos(\psi - \delta) + \sqrt{R^2 - (n^2 + m^2)\sin^2(\psi - \delta)})^2} d\psi) \end{aligned} \tag{12}$$

$J_1$  is a function of six variables. In the engineering practice,  $l_0$  and  $R$  are constant after the optical system is determined.  $m$  and  $n$  respectively represent the coordinates of pixels on the surface; Both  $k$  and  $\alpha$  are parameters of the shutter mechanism. Eq. (12) can be used to obtain the original function by Newton-Leoniz formula, but the process is quite complex, so it can be obtained by combining the Newton-Simpon formula in the numerical method:

$$\begin{aligned}
 J_1(l_0, R, m, n, k, a) = & \frac{1}{2}LdA((\psi_2 - \psi_1) - \frac{l_0^2 h}{6}(\frac{1}{l_0^2 + (\sqrt{n^2 + m^2} \cos(\psi_1 - \delta) + \sqrt{R^2 - (n^2 + m^2)\sin^2(\psi_1 - \delta)})^2} \\
 & + \frac{1}{l_0^2 + (\sqrt{n^2 + m^2} \cos(\psi_2 - \delta) + \sqrt{R^2 - (n^2 + m^2)\sin^2(\psi_2 - \delta)})^2} \\
 & + 4 \sum_{i=0}^{n'-1} \frac{1}{l_0^2 + (\sqrt{n^2 + m^2} \cos(\psi_{i+1/2} - \delta) + \sqrt{R^2 - (n^2 + m^2)\sin^2(\psi_{i+1/2} - \delta)})^2} \\
 & + 2 \sum_{i=1}^{n'-1} \frac{1}{l_0^2 + (\sqrt{n^2 + m^2} \cos(\psi_i - \delta) + \sqrt{R^2 - (n^2 + m^2)\sin^2(\psi_i - \delta)})^2})
 \end{aligned}$$

In the formula,  $n'$  is the number of shares of integral interval;  $h$  is step length.

Through the analysis of the remaining items, the value of  $n'$  can be controlled, and the precision of the engineering application can be satisfied. The above process can be accomplished by MATLAB programming.

The second part of  $J_2(l_0, R, m, n, k, a)$  can be obtained directly by integration:

$$\begin{aligned}
 J_2(l_0, R, m, n, k, a) &= \int_{\psi_1}^{\psi_2} \sin^2(\arctan(\frac{km + ka - n}{l_0 \sin(\psi) - kl_0 \cos(\psi)}))d\psi \\
 &= \frac{1}{2}LdA \int_{\psi_1}^{\psi_2} \frac{(km + ka - n)^2}{(l_0 \sin(\psi) - kl_0 \cos(\psi))^2 + (km + ka - n)^2}d\psi
 \end{aligned}$$

If the transmission ratio of the optical system is  $\tau_g$ , the luminous flux from the exit pupil to the surface  $dA'$  is as follows:

$$\begin{aligned}
 \phi_{m'n'} = \tau_g \phi = & \frac{1}{2}\tau_g LdA((\psi_2 - \psi_1) - l_0^2 \int_{\psi_1}^{\psi_2} \frac{1}{l_0^2 + (\sqrt{n^2 + m^2} \cos(\psi - \delta) + \sqrt{R^2 - (n^2 + m^2)\sin^2(\psi - \delta)})^2}d\psi) \\
 & - \frac{1}{2} \frac{\tau LdA(km + ka - n)}{\sqrt{(km + ka - n)^2 + l_0^2(1 + k^2)}}(\arctan(\frac{\sqrt{(km + ka - n)^2 + l_0^2(1 + k^2)}}{(km + ka - n)} \tan(2\psi_2 - 2\delta')) \\
 & - \arctan(\frac{\sqrt{(km + ka - n)^2 + l_0^2(1 + k^2)}}{(km + ka - n)} \tan(2\psi_1 - 2\delta'))
 \end{aligned} \tag{13}$$

It can be seen from Eq. (13) that when  $m = 0$  and  $n = 0$ , the luminous flux on the axis is equal to that of the point outside the axis. That is to say, the luminous flux on the axis is the special case of the light flux outside the axis.

The function relationship between the illuminance of the image point ( $m', n'$ ) outside the axis and the opening time of the aperture stop and the rotation angular velocity of the blade is established. When the blade opens the aperture stop, the luminance of the image point ( $m', n'$ ) outside the axis is as follows:

$$E'_{mn} = I_1(l_0, R, m', n', k, a) - I_2(l_0, R, m', n', k, a) - I_3(l_0, R, m', n', k, a) + I_4(l_0, R, m', n', k, a)$$

Among them:

$$\begin{aligned}
 I_1(l_0, R, m, n, k, a) &= \frac{1}{2} \frac{\tau_g L}{\beta^2} ((\psi_2 - \psi_1)); \\
 I_2(l_0, R, m, n, k, a) &= \frac{1}{2} \frac{\tau_g L}{\beta^2} l_0^2 \int_{\psi_1}^{\psi_2} \frac{1}{l_0^2 + (\beta\sqrt{n^2 + m^2} \cos(\psi - \delta) + \sqrt{R^2 - \beta^2(n^2 + m^2)\sin^2(\psi - \delta)})^2}d\psi \\
 I_3(l_0, R, m, n, k, a) &= \frac{1}{2} \frac{\tau L(k\beta m' + ka - \beta n')}{\beta^2 \sqrt{(k\beta m' + ka - \beta n')^2 + l_0^2(1 + k^2)}} \\
 & \arctan(\frac{\sqrt{(k\beta m' + ka - \beta n')^2 + l_0^2(1 + k^2)}}{(k\beta m' + ka - \beta n')}) \tan(2\psi_2 - 2\delta') \\
 I_4(l_0, R, m, n, k, a) &= \frac{1}{2} \frac{\tau_g L(k\beta m' + ka - \beta n')}{\beta^2 \sqrt{(k\beta m' + ka - \beta n')^2 + l_0^2(1 + k^2)}} \\
 & \arctan(\frac{\sqrt{(k\beta m' + ka - \beta n')^2 + l_0^2(1 + k^2)}}{(k\beta m' + ka - \beta n')}) \tan(2\psi_1 - 2\delta')
 \end{aligned}$$

In the opening stage of aperture stop, the light illuminance of image point ( $m', n'$ ) outside the axis is as follows:

$$E_{1m'n'} = \int_{T_0}^{T_1} E'_{mn} dt = \int_{T_0}^{T_1} I_1 dt - \int_{T_0}^{T_1} I_2 dt - \int_{T_0}^{T_1} I_3 dt + \int_{T_0}^{T_1} I_4 dt \tag{14}$$

In the full opened stage of aperture stop, the light illuminance of image point ( $m', n'$ ) outside the axis is as follows:

$$E_{2m'n'} = E'_{mn} t_1 = I_1 t_1 - I_2 t_1 - I_3 t_1 + I_4 t_1$$

In the closing stage of aperture stop, the light illuminance of image point ( $m', n'$ ) outside the axis is as follows:

$$E_{3m'n'} = \int_{T_2}^{T_3} E'_{mn} dt = \int_{T_2}^{T_3} I_1 dt - \int_{T_2}^{T_3} I_2 dt - \int_{T_2}^{T_3} I_3 dt + \int_{T_2}^{T_3} I_4 dt$$

In the shutter release cycle, the process of opening and closing the aperture stop is symmetrical, and the light illuminance of the ( $m'$ ,  $n'$ ) is as follows:

$$E_{m'n'} = 2E_{1m'n'} + E_{2m'n'} \quad (15)$$

#### 4. Experiments and analysis

After making sure of illumination function relationship of object point and image point during the process of the shutter blade rotation, combining with the sensitive property of the CCD sensor, we establish the relationship between image plane illumination and grey value of CCD sensor. The grey level of CCD sensor is shown as below:

$$DN = H \cdot R_{DN} N_g \quad (16)$$

In the Eq. (16),  $DN$  is the grey level of CCD sensor;  $H$  is the quantity of exposure on the image surface ( $\text{mJ}/\text{cm}^2$ );  $N_g$  is the gain of CCD;  $R_{DN}$  is the CCD spectral induction constant  $\text{DN}/(\text{mJ}/\text{cm}^2)$ .

The Eq. (15) is converted into the exposure quantity, and is represented to Eq. (16) to obtain the grayscale value of the target point on the camera's image surface ( $m'$ ,  $n'$ ). The expression is as follows:

$$DN_{m'n'} = t_{\text{exp}} \cdot \frac{1}{4F^2} \tau_g \tau_a \cdot \frac{E_0 \rho_A}{683\eta} \cdot R_{DN} \cdot N_g \quad (17)$$

The photoelectric measurement method detect the exposure quantity by extracting and analyzing the gray value of the image. The measuring equipment includes integrating sphere, stabilizing power supply, computer and control system.

The camera is installed to the point of the integral sphere, as shown in Fig. 9, and the shutter blade is rotated to a certain angle, as shown in Fig. 10. After integrating sphere photograph reaches heat balance, CCD sensor is controlled to photograph by use of the internal trigger mode and the images of CCD sensor is collected by computer [9]. All charge is removed before at the beginning of the CCD exposure time, to reduce the dark current and noise impact.

The gray value of the image was extracted by MATLAB [10], and the grayscale distribution of the image was obtained [11]. The grayscale values of the selected  $25 \times 10$  pixels were as shown in Table 1.

According to the grayscale value of the image, the 3D curved surface and contour plot of the image surface are drawn, which is shown in Figs. 11 and 12.

To analyze the whole working process of the shutter which controls exposure of CCD sensor, we random pick up the grey value of a pixel on the focal plane as a typical value to analyze [12]. We convert the gray value of the pixel to quantity of exposure, and draw the measurement curve which quantity of exposure changes with time, then get fitting curve of measurement data which is applied with least square method. The fitting curve is shown in Fig. 13.

In Fig. 13, the time of  $0 \sim t_1$  is the opening stage of aperture stop; the time of  $t_1 - t_2$  is the full opened stage of aperture stop; the time of  $t_2 - t_3$  is the closing stage of the aperture stop. It can be seen that the variation trend of the fitting curve is the same as that of the theoretical curve, which verifies the correctness of the analysis [13]. The value of fitting curve on the same exposure time is bigger than the value of theoretical curve. The reason is that it takes a while to shut down the integrating sphere measurement process control, which causes the actual image grey value is greater than the theoretical value [14]. According to calculating the accuracy of exposure quantity was increased by 8.9%, relative to the estimated curve.

#### 5. Conclusions

The shutter between the mirror implements that exposure time of each image point on the image surface is the same. The light energy transfer function between the eyeball and the relationship is set up. Combined with the performance parameters of the CCD sensor, the illumination of image point is accurately calculated. According to the analysis, the illumination precision of image plane improved by 8.9%, compared with the traditional algorithm. These designs improved the image clarity, and produce the high quality aerial image.

#### Acknowledgments

This work was supported by National Key Research and Development Program Funded Projects of China under Grant 2016YFC0803000.

#### References

- [1] J. Duan, X. Sun, K. Xue, Design of dynamic resolution detecting device for film type panoramic aerial camera, *Optik* 130 (2017) 1462–1468.
- [2] Sierbakov, Design and calculation of aerial camera, *Assoc. Sci. Technol. Transl. Jilin* (1985).
- [3] Z. Wang, *Photogrammetry Principle*, Surveying and mapping press, 1979.
- [4] L. Zhang, Y. Ding, H. Zhang, Adjustable exposure system for digital camera based on single curtain type shutter, *Opt. Precis. Eng.* 21 (5) (2013) 1266–1271.
- [5] C. Yu, H. Li, Design of the lens shutter mechanism in the aerial camera, *Opt. Precis. Eng.* 26 (1) (2018) 105–113.

- [6] Z. Zhuang, Finite Element Analysis and Application Based on Abaqus, Tsing Hua University Press, 2008.
- [7] J. Hu, Introduction to Optics Engineering, Dalian University of Technology Press, 2006.
- [8] C. Chen, C. Hu, W. Li, et al., Calculation method of relative illumination of lens image plane, *Acta Opt. Sin.* 36 (11) (2016) 110800101–110800112.
- [9] S. Mark, Analysis of illumination distribution in the plane of a thermal imager, *Proc. SPIE. Int. Soc. Opt. Eng.* 3061 (1997) 662–672.
- [10] W. Tu, Y. Wei, S. Shi, Application of MATLAB to digital image processing, *Microcomp. Inf.* 23 (2–3) (2007) 20–23.
- [11] J. Canny, A computational approach to edge detection, *IEEE Trans. Pattern Anal. Mach. Intell.* 8 (6) (1986) 678–679.
- [12] A. Pelamatti, V. Goiffon, A. Chabane, et al., Charge transfer inefficiency in pinned photodiode CMOS image sensors: simple Montecarlo modeling and experimental measurement based on a pulsed storage-gate method, *Solid-State Electron.* 125 (2016) 227–233.
- [13] L. Wang, G. He, X. Shen, A system for examining the imagine planes illumination nonuniformity of image-forming system on photoelectric measuring equipment using CCD, *Optoelectr. Technol.* 28 (3) (2008) 212–216.
- [14] J. Li, J. Zhao, M. Chang, et al., Radiometric calibration of photographic camera with a composite plane array CCD in laboratory, *Opt. Precision Eng.* 25 (1) (2017) 73–83.